

The Effect of Material Removal on the Corrosion Resistance and Biocompatibility of Nitinol Laser-Cut and Wire-Form Products

Jennifer Fino Decker, Christine Trépanier, Lot Vien, and Alan R. Pelton

(Submitted May 15, 2010; in revised form February 8, 2011)

Laser cutting and wire forming are two of the most commonly used processes in the manufacture of Nitinol medical devices. This study explores how varying the amount of material removed during the final surface treatment steps affects the corrosion resistance of Z-type stents that have either been laser-cut from tube or shape set from wire. All parts were subjected to a typical heat treatment process necessary to achieve an Austenite finish (A_f) temperature of 25 ± 5 °C, and were subsequently post-processed with an electrochemical passivation process. The total weight loss during post-processing was recorded and the process adjusted to create groups with less than 5%, less than 10%, and less than 25% amounts of weight loss. The parts were then crimped to 6 mm and allowed to expand back to their original diameter. The corrosion test results showed that on average both groups of Z-stents experienced an increase in the corrosion breakdown potential and a decrease in the standard deviation with increasing amounts of material removal. In addition, less material removal is required from the wire-form Z-stents as compared to the laser-cut Z-stents to achieve high corrosion resistance. Finally, 7 day nickel ion release tests performed on the wire-formed Z-stents showed a dramatic decrease from 0.0132 mg of nickel leached per day for the low weight loss group to approximately 0.001 mg/day for the medium and high weight loss groups.

Keywords biomaterials, corrosion testing, shape memory alloy

1. Introduction

Nitinol is a metallic alloy composed of near-equiatomic amounts of nickel and titanium. It exhibits extraordinarily unique properties including thermoelasticity, corrosion resistance, and biocompatibility that make Nitinol an excellent candidate for use in biomedical devices (Ref 1). The processing necessary to exploit the superelastic and shape memory properties of Nitinol involves heat treatments at temperatures most commonly ranging from 400 to 600 °C for short periods of time (2-10 min). These thermal treatments form an oxide on Nitinol, thus changing the surface chemistry and subsequent biocompatibility of the alloy.

The biocompatibility of Nitinol medical devices has always been of concern because of the known toxicity of elemental nickel present in the alloy (Ref 2). Research conducted by Trépanier et al. (Ref 3) showed that the corrosion resistance of Nitinol can be significantly improved by utilizing the proper

passivation techniques, such as electropolishing. Additional studies have gone on to prove that electropolishing provides excellent corrosion resistance in numerous biological fluids, as well as limited nickel-ion release during long-term immersion tests conducted in Hank's physiologic solution (Ref 4, 5). Because of this, electropolishing is now recognized as the gold standard for passivation of Nitinol medical devices.

After conducting a thorough literature review, it appears that limited research has been done to establish a link between the amount of material removed during the electrochemical passivation process and the biocompatibility of a device. In addition, although it is widely known that Nitinol medical devices are now manufactured utilizing both laser cutting as well as wire-forming processes, very few studies have been conducted to examine if different post-processing conditions are necessary to achieve comparable corrosion results.

This study seeks to determine whether the amount of material removed during the post-processing of Nitinol medical devices has a direct effect on their corrosion resistance and biocompatibility. Further understanding on how these passivation processes must be modified to achieve similar biocompatibility characteristics for both laser-cut and wire-form Z-stents will also be explored.

2. Experimental Methods

2.1 Materials

Superelastic Nitinol ground tube and bright wire with 50.8 at.% Ni was used to build the laser-cut and wire-form Z-stents assessed during this study. Nitinol tube, with a wall thickness of

This article is an invited paper selected from presentations at Shape Memory and Superelastic Technologies 2010, held May 16-20, 2010, in Pacific Grove, California, and has been expanded from the original presentation.

Jennifer Fino Decker, Christine Trépanier, Lot Vien, and Alan R. Pelton, Nitinol Devices and Components, 47533 Westinghouse Drive, Fremont, CA. Contact e-mail: jennifer.fino@nitinol.com.

0.455 mm, was laser-cut into a generic Z-stent pattern. The as-cut devices were then expanded using a typical stent expansion process, involving multiple heat treatments on mandrels, to achieve a final outer diameter of 28 mm. A tuning step was added to increase the A_f to 25 ± 5 °C. The wire-form Z-stents were manufactured from 0.450 mm wire. The wire forms were shape set on a fixture using similar process conditions as the laser-cut devices to reach the same final outer diameter and A_f temperature. Both the laser-cut and the wire-form Z-stents underwent varying amounts of an electrochemical passivation process in order to create groups with less than 5%, less than 10%, and less than 25% amounts of weight loss. After the passivation process, the stents were crimped onto a 6 mm pin and allowed to return to their original diameter to simulate being loaded into a delivery system and subsequently deployed.

2.2 Corrosion Testing

An EG&G Princeton Applied Research potentiostat model 273A was used to conduct the potentiodynamic polarization corrosion tests in accordance with ASTM F2129-08 (Ref 6). The potentiostat was controlled by a computer with Electrochemistry PowerSuite corrosion test software. A saturated calomel electrode (SCE) was used as a reference electrode for the potential, while two platinum auxiliary electrodes were used as the counter electrodes. All the samples were tested in an appropriate polarization cell filled with Phosphate Buffered Saline (PBS) solution with a pH of 7.4. A water bath maintained the test solution at a temperature of 37 ± 1 °C. The PBS was de-aerated for 30 min prior to immersion of the test sample, as well as throughout the test. The open circuit potential (OCP) was monitored for 1 h, followed by polarization of the sample at a voltage scan rate of 0.167 mV/s. The reverse scan was waived to locate any pit initiation sites. Each device tested was characterized by both its rest potential (E_r) and breakdown potential (E_b). In the event that the device did not experience pitting during the corrosion test and instead reached oxygen evolution without breakdown of the oxide layer, $E_{ox\ ev}$ was recorded. Three to twelve samples were corrosion tested per weight loss group for both the laser-cut and the wire-form Z-stents. The sample size was increased for those groups that had a wide range of breakdown values, to determine if any were outliers. Box plots were then created in MiniTab using both the breakdown and the oxygen evolution potentials.

2.3 Surface Characterization

The Z-stents were imaged under a Quanta200 3D DB Magnum Scanning Electron Microscope (SEM) to differentiate how additional processing affected the surface features of both the laser-cut and the wire-form devices. In addition, the oxide thickness of one wire-form Z-stent from each weight loss group was characterized using Auger Electron Spectroscopy (AES).

2.4 Nickel Ion Release Test

Three wire-form samples from each weight loss group were placed in an appropriate amount of PBS solution. The volume of solution was such that there was 1 mL of solution for every 1 cm^2 of surface area exposed and so that the samples were fully immersed. The devices were allowed to leach in PBS for 7 days at 37 °C under static conditions. At the end of 7 days, an ICP-MS instrument was used to quantify the amount of nickel released from the samples.

3. Results and Discussion

The laser-cut Z-stents post-processed with less than 5% weight loss exhibited a wide range of corrosion values leading to an average breakdown potential of 630 mV v. SCE and a standard deviation of 319 mV v. SCE. Three of the devices from this group did not experience breakdown at all. A total of nine samples were tested from this group, with none of the values appearing to be outliers. The less than 10% weight loss group had an average breakdown potential of 609 mV v. SCE, with eight out of twelve devices reaching oxygen evolution without breakdown of the oxide layer. All three of the laser-cut Z-stents from the group with the highest weight loss did not result in any corrosion damage. Table 1 summarizes the corrosion parameters for the laser-cut Z-stents. In general, the average breakdown potential of the laser-cut Z-stents increased and the standard deviation of the corrosion breakdown values decreased as more material was removed during the passivation process.

The corrosion resistance of the wire-form Z-stents also increased as the post-processing weight loss increased, following the same trend as the laser-cut Z-stents. Typical polarization curves from the wire-form group of Z-stents are shown in Fig. 1.

All the stents from the low weight loss group experienced pitting, with the average breakdown potential being 176 mV v. SCE and all three devices from the high weight loss group reached oxygen evolution without breakdown of the oxide layer. The group with less than 10% weight loss had five out of

Table 1 Corrosion parameters for laser-cut Z-stents

Amount of weight loss, %	Average E_b , mV v. SCE	Standard deviation, mV v. SCE	# of devices tested	# of devices that reached $E_{ox\ ev}$
<5	630	319	9	3
<10	609	211	12	8
<25	1101	11	3	3

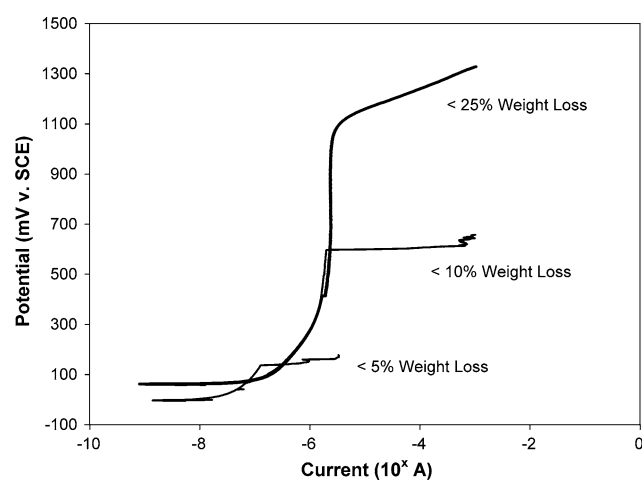
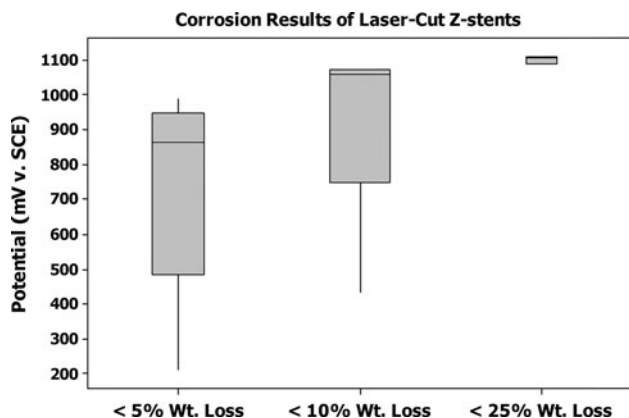
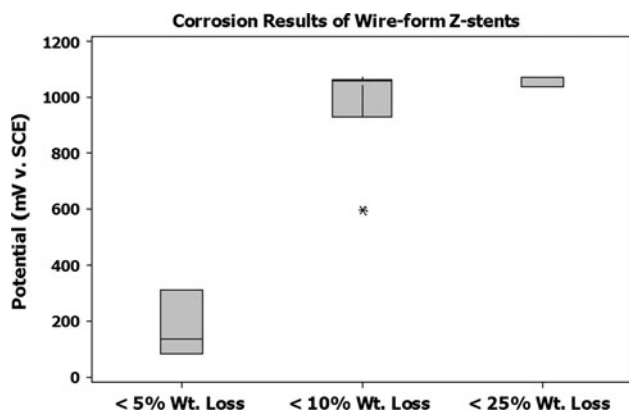


Fig. 1 Typical polarization curves of wire-form Z-stents manufactured with low, medium, and high amounts of weight loss. On average, the corrosion resistance tended to increase with larger amounts of weight loss. A similar trend was observed for the laser-cut Z-stents

Table 2 Corrosion parameters for wire-form Z-stents

Amount of weight loss, %	Average E_b , mV v. SCE	Standard deviation, mV v. SCE	# of devices tested	# of devices that reached $E_{ox\ ev}$
<5	176	120	3	0
<10	597	n/a	6	5
<25	1062	19	3	3

**Fig. 2** Variation in corrosion results as a function of weight loss for the laser-cut Z-stents. This data includes both breakdown and oxygen evolution potentials**Fig. 3** Variation in corrosion results as a function of weight loss for the wire-form Z-stents. This data includes both breakdown and oxygen evolution potentials

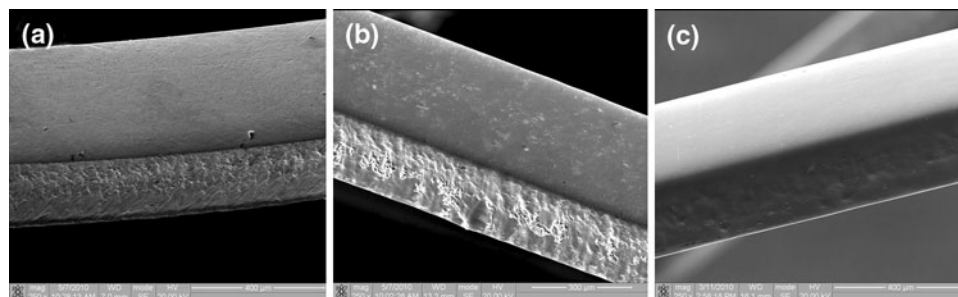
six devices reach oxygen evolution. One of the stents experienced pitting at 597 mV v. SCE. Because of the small sample size, it cannot be confirmed whether this is a real result or an outlier. Table 2 summarizes the corrosion results for the wire-form Z-stents.

Although the overall trend of increasing corrosion resistance with increasing amounts of material removal was applicable to both the laser-cut and the wire-form Z-stents, there were some important differences to note in the results. Figures 2 and 3 are box plots that illustrate the variability in corrosion results within each weight loss group for the laser-cut and wire-form product forms, respectively. Both breakdown potentials (E_b) and oxygen evolution potentials ($E_{ox\ ev}$) were included in the box plots.

The laser-cut Z-stents experienced more variability in the corrosion values within the low and medium weight loss groups than did the wire-form devices. After increasing the material weight loss to less than 25%, the variability for both product forms significantly decreased. Furthermore, it was discovered that with the exception of the one datum point, the wire-form Z-stents required less material removal than the laser-cut devices to consistently achieve oxygen evolution. Since the manufacturing processes of these two devices were paralleled in every way from shape setting through passivation, this difference must be related to the laser-cutting process. It is widely known that laser cutting creates a heat affected zone (HAZ) of recast material that if not completely removed can lead to poor fatigue results (Ref 7). This study shows that the HAZ may also play a part in the degradation of corrosion and biocompatibility of the device if not fully dissolved. Further study in this area is planned to determine exactly how much HAZ remains after varying the amount of post-processing weight loss.

An SEM analysis of both the laser-cut and the wire-form Z-stents also showed significant differences in the surface condition of the two product forms after various amounts of post-processing. Figure 4 shows a series of SEM images that depict how both the external and lateral faces of the laser-cut device become smoother as more material is removed. Because laser cutting modifies the sidewall of the stent by creating a region of HAZ, the sidewall is much rougher than what is observed on a simple wire-form device. Even at an intermediate amount of weight loss, although the external face of the Z-stent appears smooth, the as-cut sidewall still exhibits a significant amount of roughness.

A similar image progression for the wire-form Z-stents is shown in Fig. 5. For these devices, draw lines present on the surface of the wire are smoothed out with additional post-processing. Because the draw lines are found consistently

**Fig. 4** Scanning electron microscope images showing the lateral and external faces of laser-cut Z-stents electrochemically processed with (a) <5%, (b) <10%, and (c) <25% weight loss

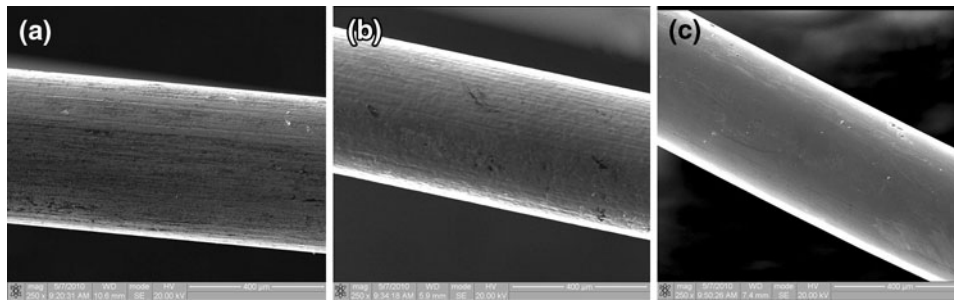


Fig. 5 Scanning electron microscope images showing wire-form Z-stents electrochemically processed with (a) <5%, (b) <10%, and (c) <25% weight loss

Table 3 Oxide thickness and nickel ion release data

Weight loss group, %	Oxide thickness, nm	Amount of Ni released, mg/day
<5	216	0.0132
<10	3.7	0.00098
<25	6.0	0.0012

around the circumference of the wire, as opposed to just being present on one face of the device as was observed for the laser-cut Z-stents, more uniform processing appears possible even at an intermediate amount of weight loss. The surface condition of the both the laser-cut and the wire-form devices correlates well with the differences in corrosion values observed. Smoother surface finishes seem to result in higher corrosion resistance.

The wire-form Z-stents underwent additional characterization studies to understand how oxide thickness and biocompatibility were also affected by the amount of material removed. AES depth profiling showed a significantly thicker oxide layer for the low weight loss group as compared to the medium and high weight loss groups. The nickel-ion release data followed a similar trend where the devices from the <5% weight loss group leached ten times more nickel per day than the other two weight loss groups. The actual oxide thickness and nickel ion release measurements are provided in Table 3. The data found in this study is consistent with the results reported by Clarke et al. (Ref 8) which also showed that thicker oxides on Nitinol resulted in elevated amounts of nickel being leached from the device during immersion testing. Previous studies on the oxidation of Nitinol have also revealed that thicker oxides are often porous and non-uniform, which could provide pathways for nickel to diffuse to the surface (Ref 9). Further characterization of the surface oxides formed on the laser-cut Z-stents and their susceptibility to nickel leaching will be conducted to determine if similar results are observed.

It is suspected that larger amounts of weight loss result in higher and more consistent corrosion resistance because a more uniform oxide layer, devoid of nickel, has been created on the surface. Previous studies have shown that for Nitinol to achieve superior corrosion resistance, uniformity of the oxide layer is extremely critical (Ref 3). Typical heat treatments on Nitinol, such as those performed in this study, are known to create an outer layer of titanium oxide, with layers of mixed oxides and nickel-rich phases beneath them (Ref 9, 10). If not enough material is removed during post-processing, areas of nickel may be exposed to the test solution resulting in lower breakdown

potentials, as well as nickel ion release. Furthermore, non-uniform and thick surface oxide layers, such as those observed on the laser-cut sidewall in Fig. 4(a) and (b), are also more susceptible to cracking during the simulated crimping and deployment of these stents. The thinner oxides created during the passivation process are purer, more protective and have the ability to flex when strained leading to exceptional biocompatibility (Ref 11).

4. Conclusions

This study examined the important relationship between the amount of material removed from a laser-cut or wire-formed Nitinol device and the biocompatibility of each device. In both cases, the corrosion behavior of the Z-stents manufactured improved and was more consistent with higher amounts of weight loss. It was also discovered that wire-form Z-stents required less material removal than its laser-cut counterparts since removal of a HAZ was unnecessary. Further characterization of the wire-form Z-stents showed that more material removal led to a thinner, more uniform oxide layer that released fewer nickel ions during a seven day immersion in a physiological solution. Based on these results, when optimizing processes for wire formed or laser-cut implant devices, it is imperative that enough material be removed to improve resistance to localized corrosion (pitting) and minimize nickel ion release. Although general weight loss guidelines have been provided, corrosion tests should always be performed on finished devices to ensure consistent corrosion resistance.

References

1. T. Dureig, A.R. Pelton, and D. Stoeckel, An Overview of Nitinol Medical Applications, *Mater. Sci. Eng. A*, 1999, **273–275**, p 149–160
2. H.G. Seiler, H. Sigel, and A. Sigel, Ed., *Handbook on Toxicity of Inorganic Compounds*, Marcel Dekker, Inc, New York, 1988
3. C. Trépainier, M. Tabrizian, L.H. Yahia, L. Bilodeau, and D.L. Piron, Effect of Modification of Oxide Layer on NiTi Stent Corrosion Resistance, *J. Biomed. Mater. Res. B*, 1998, **43(4)**, p 433–440
4. B.G. Pound, The Electrochemical Behavior of Nitinol in Simulated Physiological Solutions, *J. Biomed. Mater. Res. A*, 2008, **85A(4)**, p 1103–1113
5. B. Thierry, M. Tabrizian, C. Trépainier, O. Savadogo, and L.H. Yahia, Effect of Surface Treatment and Sterilization Processes on the Corrosion Behavior of NiTi Shape Memory Alloy, *J. Biomed. Mater. Res. A*, 2000, **51(4)**, p 685–693

6. "Standard Test Method for Conducting Cyclic Potentiodynamic Polarization Measurements to Determine the Corrosion Susceptibility of Small Implant Devices," F 2129-08, Annual Book of ASTM Standards, Vol 13.01, ASTM
7. Z.C. Lin and A. Denison, Nitinol Fatigue Resistance—A Strong Function of Surface Quality, *Med. Device Mater., Proc. Mater. Processes Med. Devices Conf.*, Sanjay Shrivastave, Ed., Sep 8-10, 2003 (Anaheim, Calif), ASM International, 2004, p 205–208
8. B. Clarke, W. Carroll, Y. Rochev, M. Hynes, and D. Bradley, Plumley, Influence of Nitinol Wire Surface Treatment on Oxide Thickness and Composition and its Subsequent Effect on Corrosion Resistance and Nickel Ion Release, *J. Biomed. Mater. Res. A*, 2006, **79A**(1), p 61–70
9. L. Zhu, J. Fino, and A.R. Pelton, Oxidation of Nitinol. SMST-2003, *Proc. Int. Conf. Shape Mem. Superelastic Technol.*, A.R. Pelton and T. Duerig, Ed., May 5-8, 2003 (Pacific Grove, Calif), SMST Society, Inc., 2004, p 357–366
10. A.R. Pelton, A. Mehta, L. Zhu, C. Trépainier, V. Imbeni, S. Robertson, M. Barney, and A. Minor, TiNi Oxidation: Kinetics and Phase Transformations, Solid-to-Solid Transformations in Inorganic Materials 2005, Volume 2: Phase Transformations in Novel Systems or Special Materials, J.M. Howe, D.E. Laughlin, J.K. Lee, U. Dahmen, W.A. Sofka, Ed., The Minerals, Metals & Materials Society, 2005, p 1029–1034
11. C. Trépainier, L. Zhu, J. Fino, and A.R. Pelton, Corrosion Resistance of Oxidized Nitinol, SMST-2003, *Proc. Int. Conf. Shape Mem. Superelastic Technol.*, A.R. Pelton and T. Duerig, Ed., May 5-8, 2003 (Pacific Grove, Calif), SMST Society, Inc., 2004, p 367–373